Mineralogical Magazine, August 2008, Vol. 72(4), pp. 971–986

Zircon dissolution in a ductile shear zone, Monte Rosa granite gneiss, northern Italy

T. J. Dempster[1], J. C. Martin[2] and Z. K. Shipton[1]

[1] Department of Geographical and Earth Sciences, Gregory Building, University of Glasgow, Glasgow G12 8QQ, UK
[2] Present address: Department of Earth Sciences, University of Durham, Durham DH1 3HP, UK

[*Received 28 February 2008; Accepted 6 November 2008*]

ABSTRACT

The sizes, distributions and shapes of zircon grains within variably deformed granite gneiss from the western Alps have been studied. Zircon shows numerous indicators of a metamorphic response in both the host gneiss and a 5 cm wide continuous ductile shear zone, within which the zircon grain sizes range from <1 μm to >50 μm. However, the very fine grain sizes are virtually absent from grain boundaries. Within this zone, zircons consistently have more rounded and embayed margins, which are interpreted as evidence of dissolution in response to fluid influx during shearing. Zircons are preferentially located near metamorphic muscovite in both the host gneiss and the shear zone and tend to show the poorest crystal shape, indicating that fluids linked to the formation and presence of muscovite may enhance both the crystallization of zircon and its subsequent dissolution. Larger zircon crystals typically show a brittle response to deformation when adjacent to phyllosilicates, with fractures consistently perpendicular to the (001) mica cleavage. The variety of metamorphic behaviour observed for zircon indicates that it may be highly reactive in sub-solidus mid-crustal metamorphic environments.

Keywords: zircon, shear zone, metamorphism, dissolution, deformation.

Introduction

Zircon is one of the most studied accessory minerals due to its use in U-Pb age determinations, and the isotopic information that it contains is responsible for many of the major conclusions concerning the Earth's early evolution (Bowring, 1995; Amelin *et al*., 1999; Wilde *et al*., 2001; Harrison *et al*., 2008). Zircon is commonly thought of as a physically and chemically durable mineral that only reacts readily in igneous and the highest-temperature metamorphic environments (Hanchar and Hoskin, 2003; Hoskin and Black, 2000; Möller *et al*., 2003). Measured diffusion rates of trace elements in zircon (Cherniak *et al*., 1997) coupled to numerous isotopic studies (Gulson and Krogh, 1973; Möller *et al*., 2002) and the preservation of complex growth zoning (Varva, 1990) all point to its chemically robust nature. Thus, many individual zircon crystals survive incorporation in clastic sedimentary rocks and subsequent thermal events associated with metamorphism (Kröner *et al*., 1988; Anderson and Griffin, 2004). However, many recent studies have demonstrated that some zircon crystals both dissolve and crystallize in a variety of crustal conditions (Tomaschek *et al*., 2003; Dempster *et al*., 2004; Fraser *et al*., 2004; Dempster *et al*., 2008) at temperatures as low as ~250ºC (Rasmussen, 2005), and micro-structural evidence (Reddy *et al*., 2006) also questions the robust nature of some zircons during deformation.

The behaviour of zircon in low-temperature conditions appears to be strongly controlled by the amount of radiation damage that accumulates in the crystal lattice from the radioactive decay of U and Th (Ewing *et al*., 1982; Farges, 1994). Radiation-damaged (metamict) zircon is suscep-

* E-mail: Tim.Dempster@ges.gla.ac.uk
DOI: 10.1180/minmag.2008.072.4.971

tible to dissolution (Geisler *et al*., 2001) and such reactivity may trigger a variety of metamorphic responses, including the development of outgrowths (Dempster *et al.*, 2004), the crystallization of new micro-zircon (Dempster *et al*., 2008), and the *in situ* recrystallization of zircon (Hoskin and Black, 2000). The variability of the response of zircon may, in part, be controlled by the metamorphic conditions, with temperature and the presence of a fluid phase being key factors (Nasdala *et al*., 2001; Geisler *et al*., 2003). With the exception of Boullier (1980), the role that deformation plays in the ability of zircon to respond to metamorphic events is largely unknown. However, in most crustal conditions and especially those at which thermal annealing of radiation damage is inefficient, the lattice of U-rich zircon may frequently be in a relatively weakened structural condition. Metamictization of U-rich parts of the zircon may result in differential expansion of the crystal lattice (Chakoumakos *et al*., 1987; Wayne and Sinha, 1992; Lee and Tromp, 1995). This is known to cause cracking of the structurally coherent parts of the zircon structure that may be difficult to repair by simple annealing at higher temperatures. Such structural failure coupled to infiltration of fluids is likely to enhance subsequent metamorphic changes to the zircon. Similarly, it would be predicted that penetrative deformation would enhance break-up and increase the chances of dissolution of the more reactive parts of zircon, especially if the grain is already weakened by radiation damage. Although the effects of deformation on the U-Pb systematics of zircon mineral separates have been investigated previously (Sinha and Glover, 1978; Wayne and Sinha, 1992) there has been no study of the morphology of zircon in such environments.

In this study, we examine the response of zircon to penetrative deformation within a regionally metamorphosed granitic gneiss host rock. Due to the abundance of relatively U-rich zircon in granitic rocks, these rock types are often the focus for geochronological investigations (Hanchar and Hoskin, 2003). Granite typically contains relatively large (20−250 μm) strongly-zoned zircon (Hoskin and Schaltegger, 2003) with a range of U-Pb ages due to the presence of inherited zircon (Williams, 1992, 2001) incorporated from surrounding country rocks during their generation and later emplacement. Studies of mineral separates from orthogneisses often demonstrate that the metamorphic equivalents of these lithologies contain similar populations of zircon with a range of U-Pb ages (Black *et al*., 1986), although the textural location of the zircon within the granite gneiss may in part control the morphology and isotopic response of zircon to the metamorphism (Sergeev *et al*., 1995).

Geological setting

The granite gneiss of Monte Rosa forms part of the upper Penninic Nappe in the west central Alps (Dal Piaz, 2001). The orthogneiss is well exposed along the border between Italy and Switzerland at Passo Moro near Macugnaga and at this locality close to the upper margin of the granite; numerous m-scale sheets of interleaved metasedimentary rocks are present (Bearth, 1952). At Passo Moro, the original granitoid is variably deformed but typically has an augen gneiss texture with a relatively flat-lying foliation that is cut by a variety of late brittle faults and joints. The late Hercynian granitoids, dated at 272±4 Ma (Liati *et al*., 2001), were intruded into amphibolite-facies country rocks and deformed and metamorphosed during the Alpine orogeny at ~42 Ma (Lapen *et al*., 2007). Alpine metamorphism was polyphase (Hunziker, 1970) and involved an initial high-pressure event at ~10 kbar and 490ºC (Frey *et al*., 1976; Dal Piaz and Lombardo, 1986; Engi *et al.*, 2001; Keller *et al*., 2004), followed by local retrogression in greenschist-facies conditions (Hunziker, 1970; Frey *et al*., 1976). The pale grey granite gneiss contains large, up to 1 cm, porphyroclasts of Carlsbad twinned K-feldspar, set in a matrix of quartz, plagioclase, biotite and phengitic muscovite. Thin, flat-lying, ductile shear zones post-date the peak regional metamorphism and locally superimpose a strong planar fabric on the earlier granite gneiss. The latter contains a variably developed flat-lying linear fabric defined by micas (Keller and Schmid, 2001).

A sample was collected at an elevation of ~2850 m. (N 45º 59.884′ E 007º 58.862′) from across a 5 cm wide continuous ductile shear zone (Fig. 1) in an otherwise uniform area of granitic gneiss. Grain size is reduced within the central 2 cm of the shear zone and the transition between the shear zone and the unsheared host gneiss occurs over a distance of ~1.5 cm either side of the central area of the symmetrical shear zone. This structure contrasts in both scale and composition with the large, 40 m wide whiteschist shear zone in the Monte Rosa granite described by

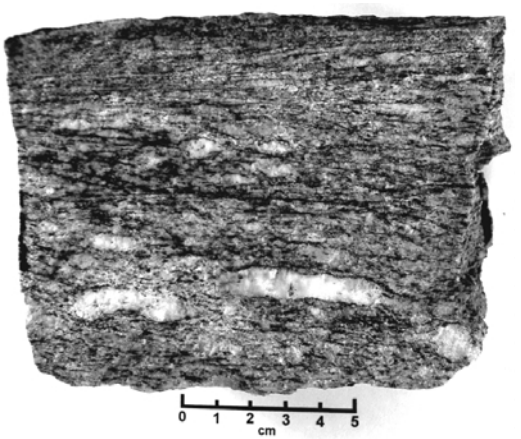

FIG. 1. Photograph of granite gneiss sample containing a fine-grained, strongly foliated, ductile, shear zone along the upper surface. Large quartz and feldspar porphyroclasts are present in the host gneiss.

Pawlig and Baumgartner (2001) in which an existing metasomatically-altered mineralized zone is thought to have been deformed.

Petrography of the sample

The granite gneiss contains zircon in both the shear zone and in the unsheared parts. The relatively sharp transition from unsheared gneiss into the ductile shear zone (Fig. 1) allows for close comparison of the zircon *in situ* within a single thin section. Analysis of the overall mineral abundance of the unsheared part of the sample shows that the granite gneiss contains quartz (35%) + plagioclase (28%) + K-feldspar (17%) + muscovite (10%) + biotite (9%) + epidote (1%) with accessory apatite, titanite, zircon and minor retrograde chlorite. In comparison, the shear zone contains significantly less K-feldspar with minor reductions in the modal amounts of quartz and plagioclase present (Fig. 2*a*, Table 2). Muscovite (26%) is strongly concentrated in the shear zone in comparison to the host gneiss. The changes in the modal mineralogy must coincide with a change in

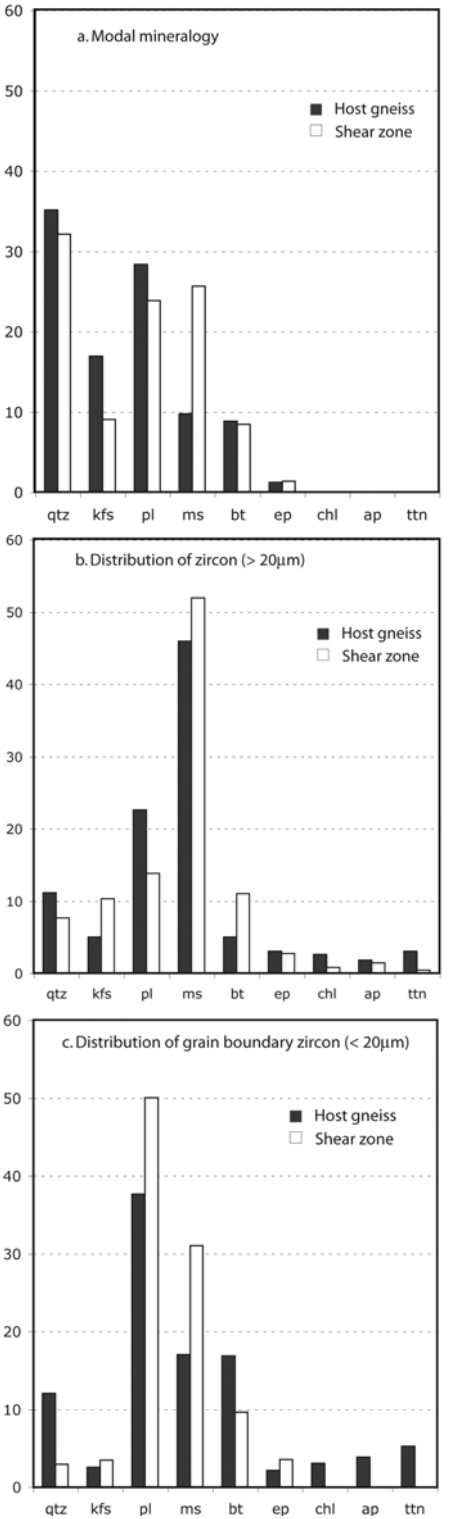

FIG. 2 (*right*). Histograms showing (*a*) modal mineralogy (%) of host gneiss and shear zone, (*b*) mineral type (%) adjacent to large zircon (>20 µm circumference) and (*c*) mineral type (%) adjacent to small zircon (<20 µm circumference) on grain boundaries. Mineral abbreviations here and elsewhere are from Kretz (1983).

composition from the host gneiss to the shear zone that principally involves hydration of the original assemblage with some loss of alkalis and silica.

The unsheared granite gneiss has a granoblastic texture with a generally uniform grain size (~200 μm) in the quartzo-feldspathic matrix. The fabric in the granite gneiss becomes more prominent as the rock is increasingly deformed into the shear zone. Mica, which most obviously defines this fabric, is progressively rotated to become parallel to the overall trend of shear zone, although there is not a large angular discordance (10–20º) between the dominant fabrics of the shear zone and the host gneiss (Fig. 1). Both quartz- and feldspar-rich parts of the gneiss generally form large elongate (~mm- to cm-scale) lens-shaped aggregates aligned parallel to the fabric of the rock. Within these lenses, isolated larger (~500 μm) grains of quartz and K-feldspar occur. Feldspar-rich aggregates tend to be a little finer-grained than those dominated by quartz. Two different textural forms of biotite are present in sections cut across the (001) mica cleavage. Larger 1 mm blocky crystals with more abundant inclusions are restricted to the gneiss outwith the shear zone. Aligned, finer-grained, thin (~100 μm), elongate biotite is present throughout both parts of the sample. The aligned micas, both muscovite and biotite, are typically associated with trails of fine-grained (~10–20 μm) epidote and titanite and these minerals may also be found in thin, linear vein-like alteration structures cross cutting the blocky biotite. The quartz typically exhibits undulose extinction associated with subgrain formation, and the presence of strained quartz generally increases towards the shear zone. In the host granite gneiss, plagioclase shows zoning in cathodoluminescence, with dark, weakly luminescent cores, but this zoning is less evident within the finer-grained shear zone. K-feldspar frequently has microcline twinning, especially around margins of the larger grains. Apatite is typically subhedral and may form large grains up to 500 μm. These larger grains often show minor fracturing particularly around their edges in response to the deformation, although the resulting fragments never appear to be dispersed more than a few microns from their parent crystal. Apatite also occurs as smaller (<50 μm), typically euhedral grains, and both large and small crystals show simple broadly concentric zoning patterns in cathodoluminescence. There is minor alteration of the granite gneiss where biotite has been partially chloritized and the edges of some quartz and feldspar grains are ragged. Both biotite and muscovite often contain small kink bands. Plagioclase frequently displays minor dusting associated with saussuritization. Although never strongly developed, small pleochroic haloes are present around some zircon inclusions in biotite.

Methods

The microtextural characteristics of zircon within both the sheared granite gneiss and the unsheared host rock were studied using an FEI Quanta 200F environmental scanning electron microscope (SEM). Two thin sections of the sample across the shear zone were examined, cut across and parallel to the plane of strain (mineral alignment), and revealed no significant difference in modal mineralogy or zircon morphology or overall shape. The bulk of the observations on zircon were made on a section cut parallel to the plane of strain. Examination of the transition zone between sheared and unsheared gneiss within the thin section was avoided because it would have introduced uncertainty as to whether the zircon should be classified as coming from sheared or unsheared gneiss. The size (long and short axes), shape and structural integrity of the zircon crystals and the nature and proportions of the adjacent minerals were recorded (Tables 1 and 2) from 1 mm^2 randomly positioned backscattered electron (BSE) images within overall areas of ~3 cm^2 in both the host rock and shear zone. A total of 25 BSE images were examined from both sheared and unsheared portions of the sample. Internal zoning of zircon was examined using cathodoluminescence images obtained with a K.E. Developments Centaurus detector attached to the SEM. Shapes were quantified by estimating the proportion of the zircon circumference dominated by planar crystal faces with a length scale varying from 10s of microns to sub-micron. Hence, in many instances we use circumference as a proxy for grain size. Anhedral margins of the zircon lack any planar crystal surfaces at any scale examined. A value of 0.1 represents an anhedral zircon with 10% planar crystal faces and 90% irregular, rounded, fragmented or embayed margins and 0.9 represents a euhedral zircon with 90% planar margins. The proportion of minerals present in the rock was determined by point counting in each part of the sample.

When fractured zircons were observed, the orientation of the principal fracture directions was

recorded relative to both the overall fabric in the rock and the orientation of the (001) cleavage in adjacent phyllosilicates. In the analysis that follows, such fractured grains are counted as single crystals including any small fragments that appear to have broken off from their original parent grains.

Results

A total of 155 individual zircons were examined in the course of this investigation, 95 from the unsheared host gneiss and 60 from the shear zone. Zircon has an overall concentration in the entire sample of 0.04 vol.%. Although the concentrations of zircon are broadly similar in both the host granite gneiss and the shear zone, modal percentages are significantly influenced by the presence of one or two larger zircon grains, even given the large number of individual zircons examined. The zircon crystals often form slightly elongate grains, with aspect ratios of 1.5:1–2:1, and are oriented with long axes either parallel to, or at a small angle to, the fabric of the rock.

The distribution and size of zircon

Zircon is present throughout the unsheared granite gneiss as small grains that range in their longest dimension from <1 μm to ~80 μm (Table 1). The overall population is dominated by large numbers of very small zircons (Fig. 3) that are atypical of those frequently reported in unmetamorphosed granite (Hoskin and Schaltegger, 2003). This grain-size distribution cannot be explained by a 3-D cut effect of a single population of larger crystals (cf. Cashman and Marsh, 1988), although thin section analysis will inevitably skew the grain-size distribution towards slightly finer grain sizes. Very few highly elongate zircon crystals are observed. Hence the crystal size distribution (Fig. 3) closely matches the true size of zircon present. Zircons are present both on grain boundaries and as apparently isolated inclusions, which are rarely observed within quartz and K-feldspar and are more commonly preserved in the other minerals (Table 2). In comparison to zircons located on grain boundaries, the grain-size distribution is shifted to finer grain size for those grains found as inclusions both within the host granite gneiss and the shear zone. The smallest zircons are those preserved within apatite and epidote in the host granite gneiss. Relative to the modal proportions of minerals in the host, small zircons appear to be preferentially concentrated within these minerals and plagioclase.

The overall number of zircon grains is reduced within the shear zone and the smallest zircons (<2 μm diameter) are virtually absent (Table 1, Fig. 3). This is reflected in the median grain size of zircon in each part of the sample. The typical zircon size in the host, as inclusions or on grain boundaries is 2 μm or 4 μm respectively, whereas those in the shear zone are 3.5 μm and 5 μm respectively. The zircons within the shear zone appear to be most strongly associated with muscovite and to a lesser extent plagioclase (Fig. 2*b*,*c*). This can only be partly explained by the greater modal abundance of muscovite in the shear zone relative to the host gneiss (Fig. 2*a*,

TABLE 1. Zircon grain size, shape and abundance as a function of location.

	Average zircon shape* (number of zircons)			
	Unsheared host gneiss		Shear zone	
Zircon size (μm^2)	Inclusions	Grain boundaries	Inclusions	Grain boundaries
0–4	0.77 (16)	0.61 (15)	0.62 (4)	0.10 (2)
4–16	0.69 (7)	0.56 (20)	0.54 (9)	0.32 (12)
16–36	0.71 (7)	0.59 (7)	0.47 (4)	0.41 (10)
36–64	– (0)	0.55 (6)	0.50 (3)	0.27 (4)
64–100	0.80 (1)	0.58 (5)	– (0)	0.33 (3)
>100	– (0)	0.40 (11)	0.60 (1)	0.21 (8)
Zircon location	Unsheared	Sheared	Average	
Inclusion	0.74±0.18 (31)	0.54±0.21 (21)	0.66 (52)	
Grain boundary	0.55±0.24 (64)	0.30±0.18 (39)	0.46 (103)	

*Shape is given on a scale of 0.1 (anhedral) to 0.9 (euhedral); (0) indicates no shape measurement.

TABLE 2. Mineralogical control on zircon distribution and shape.

Host gneiss									
	Qtz	Kfs	Pl	Ms	Bt	Ep	Chl	Ap	Ttn
Modal %	35.1	16.9	28.3	9.7	8.8	1.2	–	–	–
Estimate of total area of zircon in contact with different minerals (%)									
Zircon >20 μm	11.1	5.0	22.6	45.9	5.0	3.0	2.6	1.8	3.0
GB zircon <20 μm	12.0	2.5	37.6	17.0	16.8	2.1	3.0	3.8	5.2
Shear zone									
	Qtz	Kfs	Pl	Ms	Bt	Ep	Chl	Ap	Ttn
Modal %	32.1	9.0	23.8	25.6	8.4	1.3	–	–	–
Estimate of total area of zircon in contact with different minerals (%)									
Zircon >20 μm	7.6	10.3	13.8	51.9	11.0	2.7	0.8	1.4	0.4
GB zircon <20 μm	2.9	3.4	50.0	31.0	9.6	3.5	0.0	0.0	0.0
Zircon shapes (n = no. of zircons examined in host/shear zone)									
Zircon inclusions	0.88 (4/1)	0.60 (3/1)	0.59 (5/6)	0.50 (5/9)	0.69 (4/3)	0.83 (2/1)	0.70 (1/0)	0.86 (7/0)	–
Grain boundary zrn	0.47 (14/12)	0.42 (2/7)	0.48 (26/18)	0.37 (27/20)	0.53 (13/8)	0.48 (6/5)	0.44 (4/1)	0.65 (6/2)	0.57 (11/1)
Zircon shapes associated with particular textural/mineralogical positions									
	$Pl_{(incl)}$	$Pl_{(poly\text{-}GB)}$	$Pl_{(mono\text{-}GB)}$	$Ms_{(incl)}$	$Ms_{(poly\text{-}GB)}$	$Ms_{(mono\text{-}GB)}$	Ms-Pl $_{(GB)}$	Ms-Qtz $_{(GB)}$	
Total	0.59±0.18	0.48±0.24	0.48±0.22	0.50±0.23	0.49±0.29	0.18±0.09	0.52±0.19	0.32±0.15	
Host	0.60±0.19	0.57±0.21	0.57±0.21	0.58±0.24	0.56±0.21	0.17±0.08	–	–	
Shear zone	0.58±0.18	0.35±0.21	0.32±0.13	0.46±0.22	0.29±0.16	0.18±0.12	–	–	

Zircon size measured by estimated circumference of grain. GB = Grain boundary
Subscript incl refers to zircon inclusion in a single mineral; poly-GB refers to polyphase grain boundaries adjacent to zircon; mono-GB refers to grain boundaries with a single phase adjacent to zircon.
Qtz: quartz; Kfs: K-feldspar; Pl: plagioclase; Ms: muscovite; Bt: biotite; Ep: epidote; Chl: chlorite; Ap: apatite; Ttn: titanite

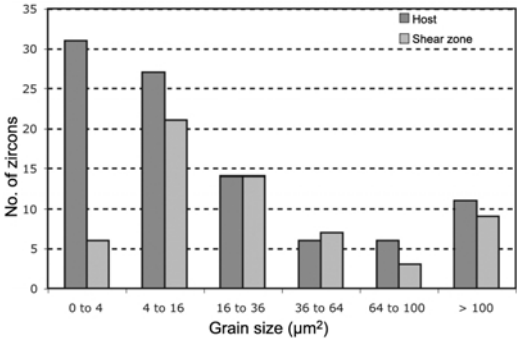

FIG. 3. Grain-size (μm^2) distribution in host-granite gneiss and ductile shear zone.

Table 2). The distribution of the finer- and coarser-grained zircon is fundamentally different (Fig. 2*b*,*c*). Thus ~50% of the larger zircons (with >20 μm circumference) are in contact with muscovite, whereas only ~20% of the smaller zircons are in contact with muscovite. However, the distribution of both zircon grain sizes in terms of adjacent minerals is very different to the overall modal proportion of minerals in the sample (Fig. 2). Irrespective of grain size, plagioclase, muscovite, biotite and epidote are preferentially associated with zircon, whereas quartz and K-feldspar consistently lack adjacent zircon (Fig. 2, Table 2).

The morphology of zircon and internal zoning

Zircon varies from very well shaped grains to those dominated by rounded, irregular and embayed margins. The large zircons may have a range of different shapes from those that have well developed crystal faces to those characterized by fractured (Fig. 5*a*–*e*) or rounded surfaces and smooth rounded embayments (Fig. 5*b*,*c*). No well shaped outgrowths of zircon are observed. Larger zircon grains typically display euhedral concentric oscillatory growth zones in cathodoluminescence, although discontinuous rims often show simpler zoning characterized by bright luminescence (Fig. 6). The oscillatory zoning is truncated by fractured and embayed margins of zircon and by the brightly luminescent zircon rims. The inner margins of the rims may be embayed (Fig. 6*a*). The smallest zircon grains (Fig. 7) lack oscillatory zoning and show only simple zoning with a brightly luminescent rim around a darker core, although clear imaging of such zoning is difficult due to their size. The shear zone contains a lower proportion of euhedral zircon, thus mean zircon shape values are greater than, and typically outwith the 1σ error of, those for zircons from equivalent textural positions in the host gneiss (Table 2, Fig. 4). This is especially so for those grains located on grain boundaries where there is a high proportion of

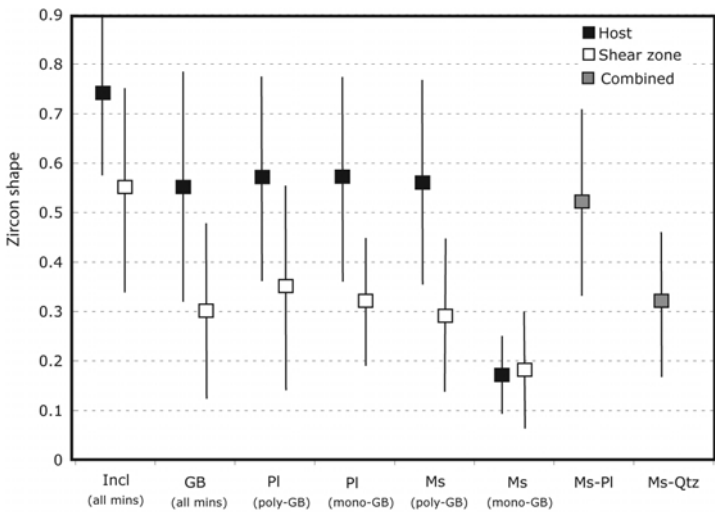

FIG. 4. Variation in zircon shape (mean and standard deviation) as a function of adjacent mineralogy and textural position within sample. Incl = zircon inclusion; GB = zircon on grain boundary; Pl (poly-GB) = zircon adjacent to plagioclase and other mineral phases; Pl (mono-GB) = zircon adjacent only to plagioclase grains. Ms-Qtz = zircon adjacent to muscovite and quartz.

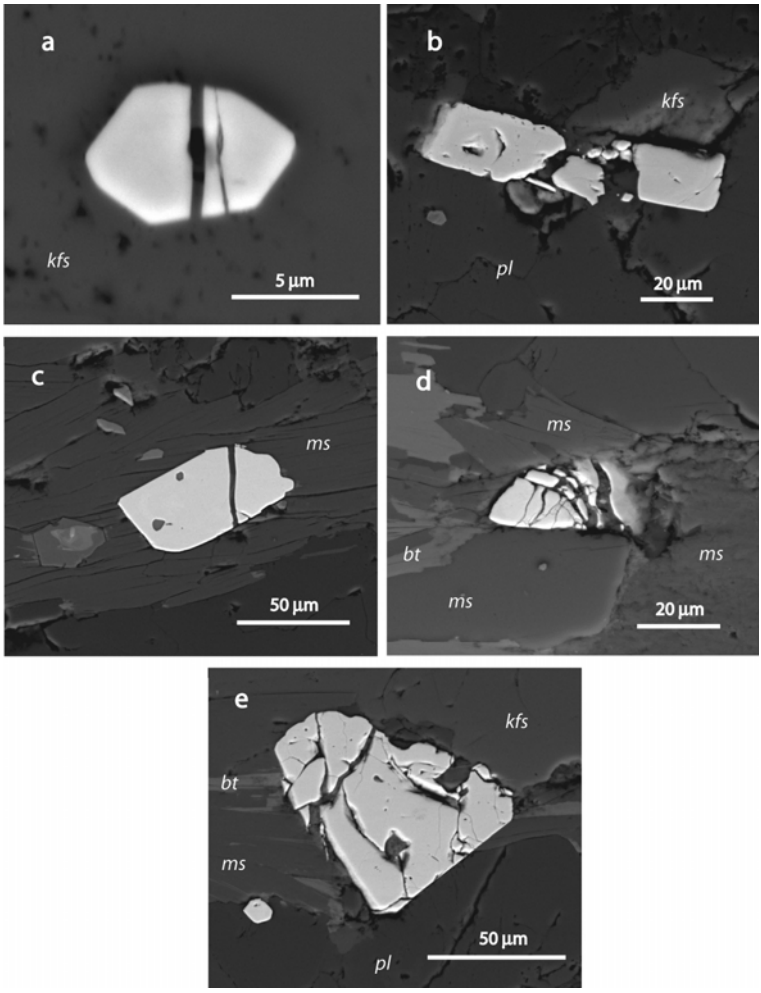

FIG. 5. BSE images of large fractured zircons from host granite gneiss (*a*, *b*) and ductile shear zone (*c*, *d*, *e*). (*a*) zircon inclusion within K-feldspar; (*b*–*e*) zircon on grain boundaries. Main cleavage oriented E–W in all images.

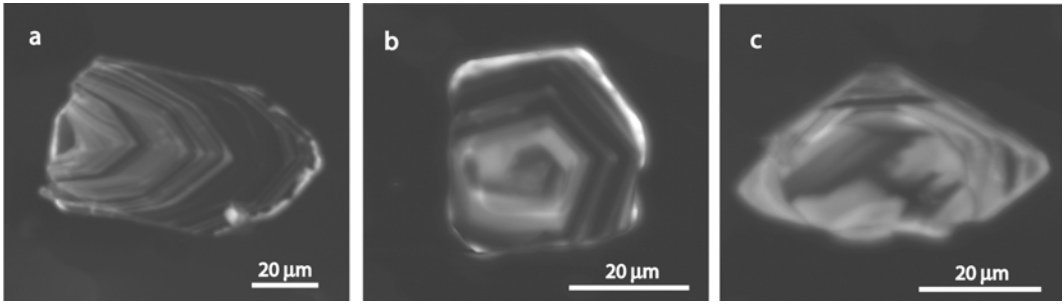

FIG. 6. Cathodoluminescence images of zircons from the ductile shear zone showing oscillatory growth zoning truncated by, (*a*) fractured margins of grain, (*b*) brightly luminescent rim and (*c*) embayed grain boundary.

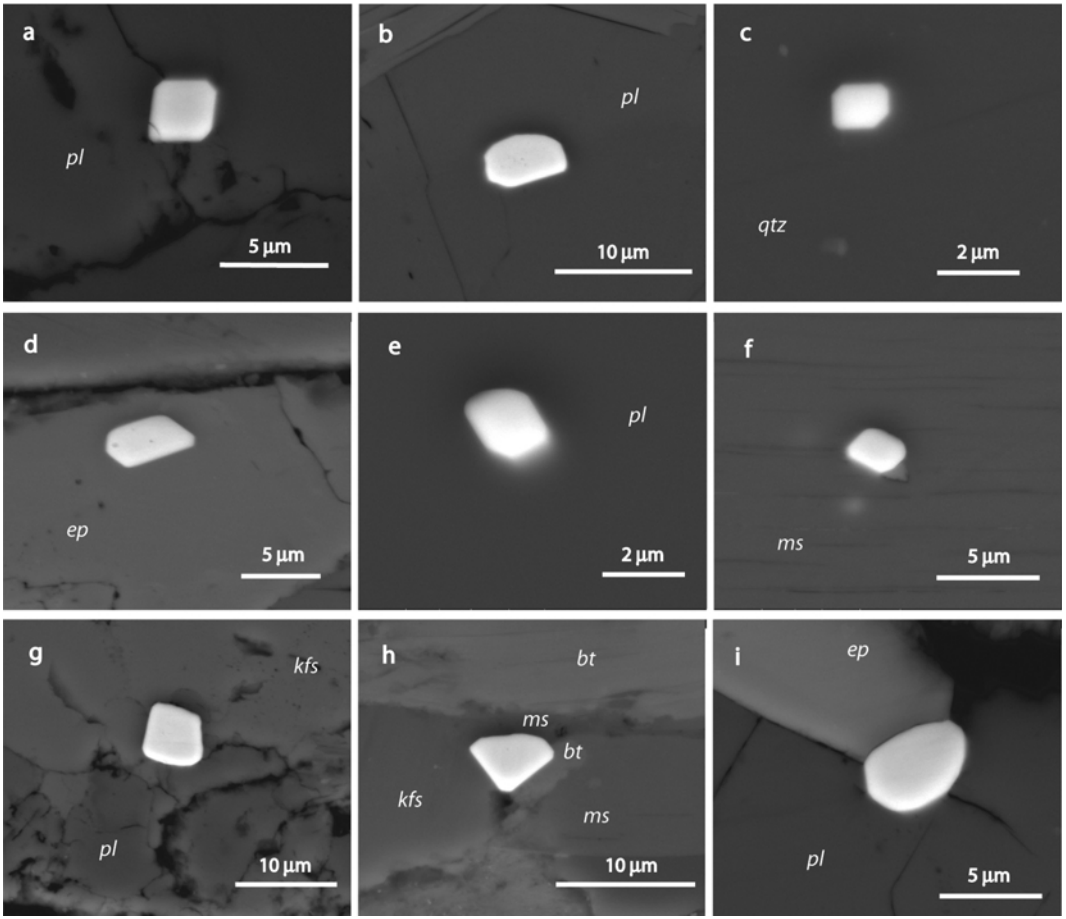

FIG. 7. BSE images of micro-zircons from granite gneiss host rock (*a*, *b*) and ductile shear zone (*c*–*i*). Zircons on grain boundaries (*a*, *g*, *h*, *i*). Zircon inclusions in various silicates (*b*–*f*).

grains with rounded surfaces (Figs 7*g*–*i*, 8*c*–*e*, Table 2). Zircon shape shows a weak correlation with adjacent mineral type such that, irrespective of their location relative to the shear zone, those solely adjacent to muscovite grain boundaries consistently show embayed or rounded margins (Fig. 4). Individual zircon grains may display both euhedral crystal faces and others with poorly developed shape (Fig. 8*c*,*e*), but individual crystals typically show the same relationship as the overall population, with irregular margins adjacent to phyllosilicates (Figs 7*h*, 8*f*).

Fractured zircon is commonly observed in both the host rock and shear zone, although a slightly greater proportion of fractured grains is present in the former. Overall, ~70% of all large zircons (>10 µm long) contain prominent fractures (Fig. 5). Fractures are rarely observed in finer-grained zircons. Typically, single, clean planar fractures with gaps of <1 µm are present and these record simple tensional opening and strain of <0.05 (Fig. 5*a*,*c*). More complex fracturing is also present within some of the larger grains (Fig. 5*b*,*d*,*e*) with shear displacements and or clear separation of fragments. In the latter, stretching of individual grains is greater with extensional strain of up to 0.1 and zircon fragments tend to have more rounded edges (Fig. 5*b*) than those that record smaller displacements and/or more complex fracture systems (Fig. 5*d*). Where complex fracture systems are present, very few smaller fragments of zircon dispersed away from the host grain are observed. The dominance of relatively poorly shaped grains

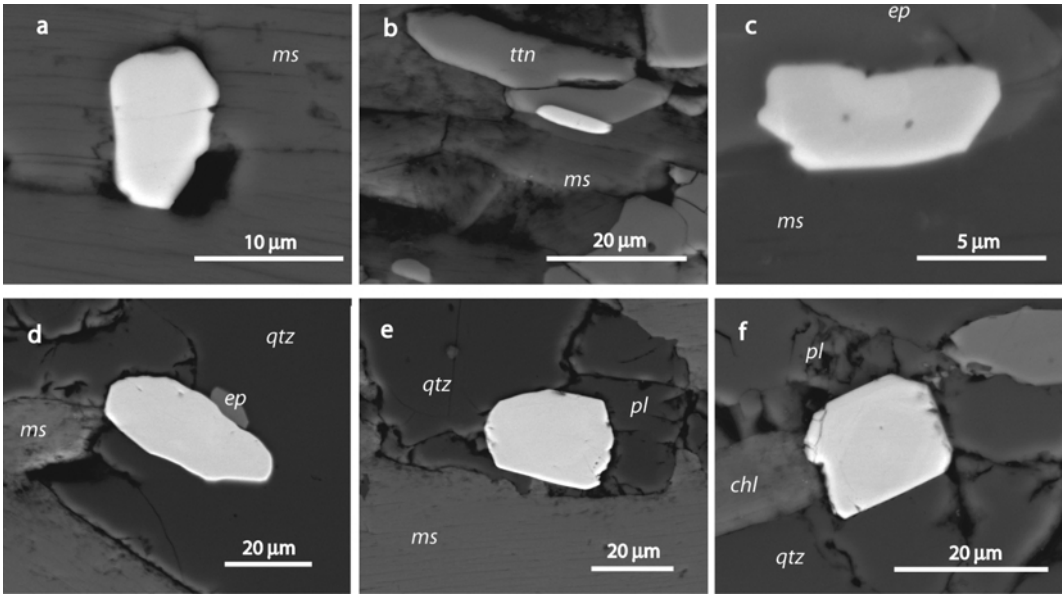

FIG. 8. BSE images of intermediate-sized zircons from host granite gneiss (*a*, *b*) and ductile shear zone (*c*– *f*). All zircons are from grain-boundary locations.

within the shear zone (Fig. 4) is due to the abundance of gently curved or rounded grain edges (Fig. 8*c*,*d*) rather than an increase in the proportion of small fragments of fractured grains. 92% of fractured grains occur adjacent to phyllosilicates (Fig. 5*c*–*e*) and the orientation of the fractures appears to be very strongly influenced by the orientation of the (001) cleavage in the adjacent micas (Fig. 9), even where the mica (001) cleavage is oriented at high angles to the dominant foliation in the rock. Overall, this results in fractures that are typically oriented perpendicular to both the main fabric in the host rock and the shear zone fabric. Secondary conjugate fractures also tend to follow a similar pattern although these show a much greater

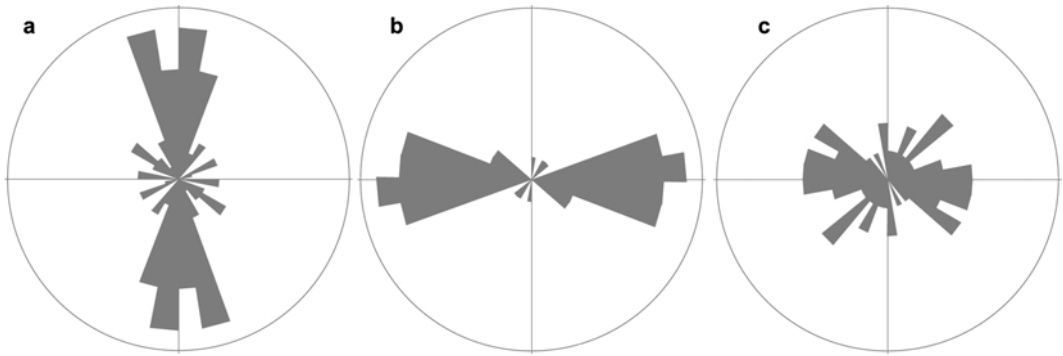

FIG. 9. Rose diagram plots showing fracture orientations within zircons from both host gneiss and shear zone: (*a*) all orientations measured relative to E–W orientation of the rock fabric in thin section (n = 62); (*b*) orientation of primary fractures measured relative to the (001) cleavage in adjacent phyllosilicate grains (n = 32, the dominant trend represents fractures at ~90º to mineral cleavage); (*c*) orientation of conjugate fractures measured relative to (001) cleavage in adjacent phyllosilicate grains (n = 30, the dominant trend represents fractures at within ~30º of orientation of mineral cleavage).

spread of orientations. The larger fractures are typically filled by a variety of newly crystallized minerals from the host rock, including biotite and feldspars. Fracture locations and orientations bear no obvious relationship to internal zoning in the zircon and commonly pass through the central parts of the zircon and are not deflected by internal planes sub-parallel to the crystal outer margins (Fig. 5*d*,*e*).

Interpretation

The majority of the larger zircons appear to be of a size, shape and possess internal zoning compatible with crystallization in a slowly cooling granitic magma (Silver and Deutsch, 1963). Hence, these are believed to represent igneous zircons that were present within an original, coarse-grained granite host rock. Such a rock is compatible with the large, twinned feldspar porphyroclasts in the gneiss and the patchy distribution of recrystallized quartz and feldspar. The distribution of the zircons is very different to that predicted from a random distribution linked to the modal mineralogy of both sheared and unsheared parts of the sample (Fig. 2). The larger zircons are strongly associated with muscovite (Fig. 2*b*) and to a lesser extent epidote. Both of these minerals formed during the metamorphism. It is uncertain whether zircon itself promotes crystallization of muscovite or perhaps more likely that the formation of muscovite is linked to the presence of other minerals that are associated with zircon. The latter would indicate that there must have been some heterogeneity in the distribution of zircons within the original granite and, due to late crystallization, zircons were concentrated on, or near, grain boundaries that subsequently acted as nucleation sites for metamorphic muscovite and epidote.

The smaller zircons have a very different distribution to the large ones, irrespective of whether they are situated in the shear zone or host gneiss (Fig. 2*b*,*c*), and this suggests that they may have a fundamentally different origin. Although still preferentially concentrated next to muscovite, this relationship is much less pronounced than with the large zircons. Small zircons are most strongly associated with adjacent plagioclase especially within the shear zone (Fig. 2*c*). This relationship either suggests that plagioclase promotes zircon stability or that other silicates such as quartz and K-feldspar enhance dissolution and hence loss of zircon. Small zircons are not typically reported from granites (Hoskin and Schaltegger, 2003), although studies of zircon commonly use mineral separates that would not sample grains of <~50 μm. Euhedral elongate micro-zircon may be found as inclusions within apatite crystals used for thermochronology studies of granites (Vermeesch *et al*., 2007). A few small zircon inclusions are preserved in apatite from the host granite gneiss, although the apparently greater concentrations in the unsheared host (Table 1) are dominated by a single large apatite containing four zircon inclusions. Apatite appears to be relatively unmodified by the metamorphic events as it retains a coarse grain size, concentric zoning, small zircon inclusions and typically good crystal form. Modal proportions of apatite are not significantly different in the shear zone compared to the host gneiss. Thus, the numerous small equant zircons in the granite gneiss are unlikely to have been released from dissolution or recrystallization of apatite host grains, although they could potentially be released from other original igneous minerals during metamorphic recrystallization.

Zircon dissolution – the influence of the ductile shear zone

The similar mineral assemblage in both host rock and shear zone suggests that the shear zone formed at temperatures close to those of peak metamorphism (~490ºC: Frey *et al*., 1976). Mineral abundances do change from the original granite gneiss into the shear zone (Fig. 2), and this seems likely to reflect an influx of fluid to form new muscovite coupled to a preferential loss or partial breakdown of other phases such as K-feldspar. If the loss of rock-forming minerals such as K-feldspar were to be solely responsible then this might generate a greater concentration of zircon within the shear zone given the perceived immobility of Zr (Pawlig and Baumgartner, 2001; Steyrer and Sturm, 2002).

The clear difference in the zircon size (Fig. 3) and consistent difference in shape of zircon in the shear zone and host gneiss (Fig. 4) suggests that deformation, either directly or indirectly, affects the morphology of zircon within the shear zone. Despite the evidence for zircon having a brittle response to deformation, fracturing is not obviously correlated with the shear-zone deformation. There is very little evidence of major shear displacement on the fractured zircon and the few small fragments of zircon that are observed associated with the fractures are not displaced significantly but are preserved immediately

adjacent to the host grain (Fig. 5*b*). Indeed, there is a general lack of either small zircon fragments, compatible with the break up of existing larger grains, or greater numbers of individual zircons within the shear zone.

A key difference between the sheared and unsheared granite gneiss is the virtual absence of abundant fine-grained euhedral zircons from the shear zone. This, coupled with the generally rounded or embayed nature of the zircons in the shear zone (Table 2, Fig. 4) and the truncation of internal zoning against embayed grain margins (Fig. 6*c*), strongly suggests that there has been greater dissolution of zircon within the shear zone. Hence, the small zircons have been preferentially lost as a consequence of dissolution. This is also compatible with the fact that zircons isolated as inclusions within the rock-forming minerals are typically euhedral in comparison to those on grain boundaries (Table 2). Many inclusions have probably been protected from exposure to fluids and generally have retained good crystal surfaces. Consequently, zircons in the shear zone have been able to dissolve in a metamorphic fluid that moved through the shear zone, either at the time of shear-zone formation or subsequently. Within the shear zone, the zircons trapped as inclusions within other minerals are relatively rounded in comparison to those in the unsheared gneiss. This indicates that some recrystallization of the silicates must take place after zircon dissolution, and it seems that at least some part the dissolution history must have occurred at elevated temperature, perhaps synchronous with the ductile deformation.

Zircon fracturing and growth – the influence of regional metamorphism

Deformation in the parent gneiss has had a direct influence on some of the larger zircons and may point to a link between grain size and material strength (Sammis *et al*., 1987). Fractures within zircons are filled with high-temperature minerals such as biotite and feldspar (Fig. 5*e*). Most of the deformation has caused the fracturing without displacement (Fig. 5). This suggests that pure shear may be an important factor in formation of the ductile fabric (Butler *et al*., 2002). The lack of radial or concentric fractures within zircon (Wayne and Sinha, 1992) suggests that U-zoning and metamictization has had no influence on the zircon during deformation. This is probably due to the relatively young age of the original granite, coupled with metamorphism-annealing radiation damage prior to the deformation. The differing morphologies of fractured zircons suggest that some have experienced dissolution after brittle deformation (Fig. 5*b*) whereas others retain sharp irregular margins (Fig. 5*d*,*e*). This may relate to the timing of fracture development or alternatively to differences in fluid access.

The almost ubiquitous association of fractured zircon with adjacent phyllosilicates suggests that micas play an important role in promoting brittle failure. This might be linked to the ease with which other silicates adjacent to zircon may recrystallize and consequently change shape in response to stress. In contrast, mica shape is subject to much greater crystallographic control and may impose greater tensional forces perpendicular to the direction of shear on adjacent zircon.

The metamorphic processes responsible for forming the shear zone have influenced the size, distribution and shape of zircon, although zircon of undoubtedly igneous origin has also survived. Hence, the dissolution events were inefficient and subject to local mineralogical control but they also affected the granite gneiss prior to the shear-zone formation. Zircon shows most evidence of dissolution when adjacent to muscovite, especially when it is the only mineral adjacent to the individual zircon (Fig. 4). This local dissolution is not matched by synchronous local crystallization of zircon or Zr-rich phases. The Zr is presumably removed in the fluid phase (Schmidt *et al*., 2006) and potentially low-temperature hydrothermal zircon (Rubin *et al*., 1989) or metamorphic zircon may crystallize elsewhere. Sub-solidus metamorphic zircon has been reported in other studies but typically largely involves recrystallization of earlier zircon (Gebauer *et al*., 1997; Rubatto *et al*., 1999; Tomaschek *et al*., 2003) or new crystallization either as outgrowths on greenschist-facies zircons (Dempster *et al*., 2004) or as discrete micro-zircons in amphibolite-facies schists (Dempster *et al*., 2008). In the latter study, alternating periods of zircon dissolution and growth are inferred from the distribution of zircon with respect to porphyroblast phases. The micro-zircons in the granite gneiss could potentially have a similar metamorphic origin which predates the fabric-forming events, given that their morphology is identical to those reported by Dempster *et al*. (2008), the evidence of dissolution, the characteristic good crystal form and their inclusion within metamorphic micas

(Fig. 7*f*). The small zircons may share a growth history with thin discontinuous rims on the larger grains that may represent late outgrowths formed after a period of dissolution.

Discussion

The distribution, size and shape of zircon in the Monte Rosa granite gneiss are strongly controlled by metamorphic processes linked to ductile shearing. Similar sub-solidus changes are now recognized in a variety of rocks and point to zircon acting as a metamorphic mineral in a range of crustal environments (Rubatto *et al*., 2001; Williams, 2001; Tomaschek *et al*., 2003; Dempster *et al*., 2004; Rasmussen, 2005; Dempster *et al*., 2008). Within the sheared gneiss, dissolution is the most commonly observed response of zircon and the difference in behaviour between inclusions and those crystals on grain boundaries point to the importance of a fluid phase (Tomaschek *et al*., 2003; Geisler *et al*., 2003). Radiation damage is known to play a significant role in enhancing the solubility of zircon (Balan *et al*., 2001; Geisler *et al*., 2003). In these rocks there is a lack of evidence for radiation damage-related effects, probably due to the relatively young age of the zircon (Liati *et al*., 2001). However, the evidence of dissolution within the shear zone suggests that radiation damage within the lattice is not a requirement for significant zircon dissolution.

A control on the dissolution process appears to be the presence of muscovite. Small zircons appear to be preferentially removed when adjacent to muscovite (Fig. 2) and the shapes of zircons adjacent to muscovite are consistent with evidence of partial dissolution (Figs 4 and 7*h*). However, muscovite also appears to have a greater affinity with zircon than other rock-forming silicates, whether original igneous zircon or micro-zircon of possible metamorphic origin (Fig. 2*b*,*c*). Similar behaviour has been reported by Dempster *et al*. (2008) in amphibolite-facies mica schists and attributed to zircon solubility being buffered by the presence of F-rich fluids. However, the spatial controls on zircon dissolution within the orthogneiss suggests that either fluid composition is subject to extremely local buffering or that infiltration is restricted to certain specific mineral boundaries.

Within the shear zone, a dominant loss of zircon occurs and this is not matched by synchronous growth elsewhere in the sample. Therefore, Zr does not show closed-system behaviour and this study cautions against the assumption that Zr acts as an immobile element. The switching between precipitation and dissolution and operation of local controls does suggest that mobility of Zr might be quite restricted and so conditions suitable for metamorphic zircon growth may be found in close proximity to the shear zone. Growth of other silicates containing significant concentrations of Zr (cf. Degeling *et al*., 2001) may also occur in the vicinity.

Summary

A population of fine-grained micro-zircons is identified in the Monte Rosa granite gneiss. Such zircons are absent from a small ductile shear zone in this host rock and the morphology of the larger zircons is characterized by embayed grain margins. These observations suggest that significant dissolution of zircon occurs during the formation of the shear zone. Many zircons contain brittle fractures that relate to early fabric development in the host gneiss; however, other than the evidence for dissolution, zircon shows no structural response to deformation within the shear zone.

Acknowledgements

This study was supported by funding from the Carnegie Trust for the Universities of Scotland. Cristina Persano and Martin Lee are thanked for assistance during fieldwork, Duncan Hay for discussions on metamorphic zircon and Peter Chung and John Gilleece for technical expertise. Andreas Möller and an anomymous reviewer are thanked for their helpful comments.

References

Amelin, Y., Lee, D-C., Halliday, A.N. and Pidgeon, R.T. (1999) Nature of the Earth's earliest crust from hafnium isotopes in single detrital zircons. *Nature*, **399**, 252–255.

Andersen, T. and Griffin, W.L. (2004) Lu-Hf and U-Pb isotope systematics of zircon from the Storgangen Intrusive Complex, SW Norway; implications for the composition and evolution of Precambrian lower crust in the Baltic shield. *Lithos*, **73**, 271–288.

Balan, E., Neuville, D.R., Trocellier, P., Fritsch, E., Muller, J-P., and Calas, G. (2001) Metamictization and chemical durability of detrital zircon. *American Mineralogist*, **86**, 1025–1033.

Bearth, P. (1952) *Geologie und Petrographie des Monte Rosa*. Beiträge zur Geologischen Karte der Schweiz, 94 pp.

Black, L.P., Williams, I.S. and Compston, W. (1986) Four zircon ages from one rock: the history of a 3,930 Ma-old granulite from Mount Scones, Enderby Land, Antarctica. *Contributions to Mineralogy and Petrology*, **94**, 427–437.

Boullier, A.M. (1980) A preliminary study on the behaviour of brittle minerals in a ductile matrix: example of zircons and feldspars. *Journal of Structural Geology*, **2**, 211–217.

Bowring, S.A. (1995) The Earth's early evolution. *Science*, **269**, 1535–1540.

Butler, R.W.H., Casey, M., Lloyd, G.E., Bond, C., McDade, P., Shipton, Z.K. and Jones, R. (2002) Vertical stretching and crustal thickening at Nanga Parbat, Pakistan Himalaya: a model for distributed continental deformation during mountain building. *Tectonics*, **21**, 1–17.

Cashman, K.V. and Marsh, B.D. (1988) Crystal size distribution (CSD) in rocks and the kinetics and dynamics of crystallization. II: Makaopuhi lava lake. *Contributions to Mineralogy and Petrology*, **99**, 292–305.

Chakoumakos, B.C., Murakami, T., Lumpkin, G.R. and Ewing, R.C. (1987) Alpha-decay induced fracturing in zircon: The transition from the crystalline to the metamict state. *Science*, **236**, 1556–1559.

Cherniak, D.J., Hanchar, J.M. and Watson, E.B. (1997) Rare-earth diffusion in zircon. *Chemical Geology*, **134**, 289–301.

Dal Piaz, G.V. (2001) Geology of the Monte Rosa massif: historical review and personal comments. *Schweizerische Mineralogische und Petrographische Mitteilungen*, **81**, 275–303.

Dal Piaz, G.V. and Lombardo, B. (1986) Early Alpine eclogite metamorphism in the Penninic Monte Rosa-Gran Paradiso basement nappes of the northwestern Alps. Pp. 249–265 in: *Blueschists and Eclogites*: (B.W. Evans and E.H. Brown, editors), **164**, Geological Society of America Memoir.

Degeling, H., Eggins, S. and Ellis, D.J. (2001) Zr budgets for metamorphic reactions, and the formation of zircon from garnet breakdown. *Mineralogical Magazine*, **65**, 749–758.

Dempster, T.J., Hay, D.C. and Bluck, B.J. (2004) Zircon growth in slate. *Geology*, **32**, 221–224.

Dempster, T.J., Hay, D.C., Gordon, S.H. and Kelly, N.M. (2008) Micro-zircon: origin and evolution during metamorphism. *Journal of Metamorphic Geology*, **26**, 499–507.

Engi, M., Scherrer, N.C. and Burri, T. (2001) Metamorphic evolution of pelitic rocks of the Monte Rosa nappe: Constraints from petrology and single grain monazite age data. *Schweizerische Mineralogische und Petrographische Mitteilungen*, **81**, 305–328.

Ewing, R.C., Haaker, R.F. and Lutze, W. (1982) Leachability of zircon as a function of alpha dose. *Scientific Basis for Radioactive Waste Management*, **5**, 389–397.

Farges, F. (1994) The Structure of Metamict Zircon: A Temperature-Dependant EXAFS Study: *Physics and Chemistry of Minerals*, **20**, 504–514.

Fraser, G.L., Pattison, D.R.M. and Heaman, L.M. (2004) Age of the Ballachulish and Glen Coe Igneous Complexes (Scottish Highlands), and paragenesis of zircon, monazite and baddeleyite in the Ballachulish Aureole. *Journal of the Geological Society, London*, **161**, 447–462.

Frey, M., Hunziker, J.C., O'Neil, J.R. and Schwander, H.W. (1976) Equilibrium-disequilibrium relations in the Monte Rosa granite, western Alps: petrological, Rb-Sr and stable isotope data. *Contributions to Mineralogy and Petrology*, **55**, 147–179.

Gebauer, D., Schertl, H-P., Brix, M. and Schreyer, W. (1997) 35 Ma old ultrahigh-pressure metamorphism and evidence for very rapid exhumation in the Dora Maira Massif, Western Alps. *Lithos*, **41**, 5–24.

Geisler, T., Ulonska, M., Schleicher, H., Pidgeon, R.T. and van Bronswijk, W. (2001) Leaching and differential recrystallization of metamict zircon under experimental hydrothermal conditions. *Contributions to Mineralogy and Petrology*, **141**, 53–65.

Geisler, T., Pidgeon, R.T., Kurtz, R., van Bronswijk, W. and Schleicher, H. (2003) Experimental hydrothermal alteration of partially metamict zircon. *American Mineralogist*, **88**, 1496–1513.

Gulson, B.L. and Krogh, T.E. (1973) Old lead components in the young Bergell Massif, south-east Swiss Alps. *Contributions to Mineralogy and Petrology*, **40**, 239–252.

Hanchar, J.M. and Hoskin, P.W.O. (2003) Zircon. *Reviews in Mineralogy and Geochemistry*, **53**, Mineralogical Society of America, Washington, DC, 500pp.

Harrison, T.M., Schmitt, A.K., McCulloch, M.T. and Lovera, O.M. (2008) Early ($\geqslant$4.5 Ga) formation of terrestrial crust: Lu-Hf, $\delta^{18}O$, and Ti thermometry results for Hadean zircons. *Earth and Planetary Science Letters*, **268**, 476–486.

Hoskin, P.W.O. and Black, L.P. (2000) Metamorphic zircon formation by solid-state recrystallization of protolith igneous zircon. *Journal of Metamorphic Geology*, **18**, 423–439.

Hoskin, P.W.O. and Schaltegger, U. (2003) The Composition of Zircon and Igneous and Metamorphic Petrogenesis. Pp. 27–62 in: *Reviews in Mineralogy and Geochemistry*, **53**, Mineralogical Society of America, Washington, DC, 500pp.

Hunziker, J.C. (1970) Polymetamorphism in the Monte Rosa, Western Alps. *Eclogae Geologicae Helvetiae*, **63**, 151–161.

Keller, L.M. and Schmid S.M. (2001) On the kinematics of shearing near the top of the Monte Rosa nappe and the nature of the Furgg zone in Val Loranco (Antrona valley, N. Italy): tectonometamorphic and paleogeographical consequences: *Schweizerische Mineralogische Petrographische Mitteilungen*, **81**, 347–367.

Keller, L.M., Abart, R., Stünitz, H. and Capitani, C.D.E. (2004) Deformation, mass transfer and mineral reactions in an eclogite facies shear zone in a polymetamorphic metapelite (Monte Rosa nappe, western Alps). *Journal of Metamorphic Geology*, **22**, 97–118.

Kretz, R. (1983) Symbols for rock-forming minerals. *American Mineralogist*, **68**, 277–279.

Kröner, A., Wendt, I., Liew, T.C., Compston, W., Todt, W., Fiala, J., Vanková, V. and Vanek, J. (1988) U-Pb zircon and Sm-Nd model ages of high-grade Moldanubian metasediments, Bohemian Massif, Czechoslovakia. *Contributions to Mineralogy and Petrology*, **99**, 257–266.

Lapen, T.J., Johnson, C.M., Baumgartner, L.P., Dal Piaz, G.V., Skora, S. and Beard, B.L. (2007) Coupling of oceanic and continental crust during Eocene eclogite-facies metamorphism: evidence from the Monte Rosa nappe, western Alps. *Contributions to Mineralogy and Petrology*, **153**, 139–157.

Lee, J.K.W. and Tromp, J. (1995) Self-induced fracture generation in zircon. *Journal of Geophysical Research*, **100**, 17753–17770.

Liati, A., Gebauer, D., Froitzheim, N. and Fanning, C.M. (2001) U-Pb SHRIMP geochronology of an amphibolitized eclogite and an orthogneiss from the Furgg zone (Western Alps) and implications for its geodynamic evolution. *Schweizerische Mineralogische und Petrographische Mitteilungen*, **81**, 379–393.

Möller, A., O'Brien, P.J. and Kennedy, A. (2002) Polyphase zircon in ultrahigh-temperature granulites (Rogaland, SW Norway): constraints for Pb diffusion in zircon. *Journal of Metamorphic Geology*, **20**, 727–740.

Möller, A., O'Brien, P.J., Kennedy, A. and Kröner, A. (2003) Linking growth of zircon and metamorphic textures to zircon chemistry: an example from the ultrahigh-temperature granulites of Rogaland (SW Norway). Pp. 65–81 in: *Geochronology: Linking the Isotopic Record with Petrology and Textures*. (D. Vance, W. Müller and I.M. Villa, editors). Special Publication, **220**. Geological Society of London.

Nasdala, L., Wenzel, M., Vavra, G., Irmer, G., Wenzel, T. and Kober, B. (2001) Metamictization of natural zircon: accumulation versus thermal annealing of radioactivity-induced damage. *Contributions to Mineralogy and Petrology*, **141**, 125–144.

Pawlig, S. and Baumgartner, L.P. (2001) Geochemistry of a talc-kyanite-chloritoid shear zone within the Monte Rosa granite, Val d'Ayas, Italy. *Schweizerische Mineralogische und Petrographische Mitteilungen*, **81**, 329–346.

Rasmussen, B. (2005) Zircon growth in very low grade metasedimentary rocks: evidence for zirconium mobility at ~250ºC. *Contributions to Mineralogy and Petrology*, **150**, 146–155.

Reddy, S.M., Timms, N.E., Trimby, P., Kinny, P.D., Buchan, C. and Blake, K. (2006) Crystal-plastic deformation of zircon: A defect in the assumption of chemical robustness. *Geology*, **34**, 257–260.

Rubatto, D., Gebauer, D. and Compagnoni, R. (1999) Dating of eclogite-facies zircons: the age of Alpine metamorphism in the Sesia-Lanzo Zone (Western Alps). *Earth and Planetary Science Letters*, **167**, 141–158.

Rubatto, D., Williams, I.S. and Buick, I.S. (2001) Zircon and monazite response to prograde metamorphism in the Reynolds Range, central Australia. *Contributions to Mineralogy and Petrology*, **140**, 458–468.

Rubin, J.N., Henry, C.D. and Price, J.G. (1989) Hydrothermal zircons and zircon overgrowths, Sierra Blanca Peaks, Texas. *American Mineralogist*, **72**, 865–869.

Sammis, C., King, G. and Biegel, R. (1987) The kinematics of gouge deformation. *Pure and Applied Geophysics*, **125**, 777–812.

Schmidt, C., Rickers, K., Wirth, R., Nasdala, L. and Hanchar, J.M. (2006) Low-temperature Zr mobility: An *in situ* synchrotron-radiation XRF study of the effect of radiation damage in zircon on the element release in H_2O + HCl ± SiO_2 fluids: *American Mineralogist*, **91**, 1211–1215.

Sergeev, S.A., Meier, M. and Steiger, R.H. (1995) Improving the resolution of single-grain U/Pb dating by the use of zircon extracted from feldspar: Application to the Variscan magmatic cycle in the central Alps. *Earth and Planetary Science Letters*, **134**, 37–51.

Silver, L.T. and Deutsch, S. (1963) Uranium-lead isotopic variations in zircons: A case study. *Journal of Geology*, **71**, 721–758.

Sinha, A.K. and Glover L. (1978) U/Pb systematics of zircons during dynamic metamorphism: A study from the Brevard Fault Zone: *Contributions to Mineralogy and Petrology*, **66**, 305–310.

Steyrer, H.P. and Sturm, R. (2002) Stability of zircon in a low-grade ultramylonite and its utility for chemical mass balancing: the shear zone at Miéville, Switzerland. *Chemical Geology*, **187**, 1–19.

Tomaschek, F., Kennedy, A.K., Villa, I.M., Lagos, M.

and Ballhaus, C. (2003) Zircons from Syros, Cyclades, Greece – recrystallization and mobilization of zircon during high pressure metamorphism. *Journal of Petrology*, **44**, 1977–2002.

Varva, G. (1990) On the kinematics of zircon growth and its petrogenetic significance: A cathodoluminescence study. *Contributions to Mineralogy and Petrology*, **106**, 90–99.

Vermeesch, P., Seward, D., Latkoczy, C., Wipf, M., Günther, D. and Baur, H. (2007) α-Emitting mineral inclusions in apatite, their effect on (U-Th)/He ages, and how to reduce it. *Geochimica et Cosmochimica Acta*, **71**, 1737–1746.

Wayne, D.M. and Sinha, A.K. (1992) Stability of zircon U-Pb systematics in a greenschist-grade mylonite: An example from the Rockfish Valley Fault Zone, Central Virginia, USA: *Journal of Geology*, **100**, 593–603.

Wilde, S.A., Valley, J.W., Peck, W.H. and Graham, C.M. (2001) Evidence from detrital zircons for the existence of continental crust and oceans on the Earth 4.4 Ga ago. *Nature*, **409**, 175–178.

Williams, I.S. (1992) Some observations on the use of zircon U-Pb geochronology in the study of granitic rocks. *Transactions of the Royal Society of Edinburgh (Earth Sciences)*, **83**, 447–458.

Williams, I.S. (2001) Response of detrital zircon and monazite, and their U-Pb isotopic systems, to regional metamorphism and host-rock partial melting, Cooma Complex, southeastern Australia. *Australian Journal of Earth Science*, **48**, 557–580.